

Is a fluorescence navigation system with indocyanine green effective enough to detect liver malignancies?

Takayuki Tanaka M.D., Mitsuhsa Takatsuki M.D., PhD, Masaaki Hidaka M.D., PhD,
Takanobu Hara M.D., Izumi Muraoka M.D., Akihiko Soyama M.D., PhD, Tomohiko
Adachi M.D., PhD, Tamotsu Kuroki M.D., PhD, Susumu Eguchi M.D., PhD

Department of Surgery, Nagasaki University Graduate School of Biomedical Sciences

Running title: ICG-FNS to detect liver malignancies

List words: indocyanine green, fluorescence navigation system, liver tumor

Word count: 2811 words Figure count: 4 Table count: 1

Disclosure: The authors have no conflicts of interest or funding to disclosure.

Address correspondence to: Susumu Eguchi
Department of Surgery
Nagasaki University Graduate School of Biomedical Sciences
1-7-1 Sakamoto, Nagasaki, Japan,
zip code,852-8501
Phone: +81-95-819-7316 Fax: +81-95-819-7319
Email: sueguchi@nagasaki-u.ac.jp

Abstract

[Background] Although several reports have shown the efficacy of a fluorescence navigation system (FNS) with indocyanine green (ICG) to detect liver malignancies during hepatectomy, the real accuracy of this procedure is not yet clear. This study aimed to analyze the actual efficacy of ICG-FNS in cirrhotic and non-cirrhotic livers.

[Methods] Ten cirrhotic whole livers explanted from liver transplant recipients and twenty-three non-cirrhotic livers from patients who underwent hepatectomy for various kinds of liver tumors were investigated with ICG-FNS. All surgical specimens were analyzed macroscopically and pathologically.

[Results] In the patients with a cirrhotic liver, most nodules illuminated by ICG-FNS were diagnosed as regenerative nodules pathologically. The positive predictive value was 5.4%. There was a significant difference in positive predictive value to detect malignant liver tumors between cirrhotic liver and non-cirrhotic liver (5.4% vs 100%, $p < 0.0001$). In the non-cirrhotic livers, eleven of thirty-three (32.4%) tumors were not recognized by ICG-FNS through the liver surface before resection. There was a significant difference in the depth from the liver surface to tumor between illuminated nodules and non-illuminated nodules (1.5 mm vs 11.6 mm, $p < 0.01$).

[Conclusions] It is necessary to know the limitation of ICG-FNS when detecting liver

malignancies in both cirrhotic and non-cirrhotic livers.

Introduction

In liver surgery, in order to achieve absolute removal of tumors, it is essential to recognize even small tumors and to ensure the accurate surgical margin intraoperatively. Intraoperative ultrasonography has been the gold standard to detect liver tumors since it was introduced by Makuuchi et al.¹⁾. Recently, several reports have shown the efficacy of intraoperative navigation surgery using a fluorescence navigation system with indocyanine green (ICG-FNS)²⁾³⁾.

ICG-FNS has generally been used to detect the sentinel lymph nodes in the breast^{4) 5)}, gastric⁶⁾⁷⁾⁸⁾, lung⁹⁾¹⁰⁾, and esophageal cancers¹¹⁾ and to intraoperatively assess graft patency in vascular surgery¹²⁾¹³⁾. The adaption of ICG-FNS was expanded for hepatobiliary surgery³⁾¹⁴⁾¹⁵⁾. Ishizawa et al.²⁾ reported that fluorescence intraoperative cholangiography with ICG is a safe and valuable procedure for a road map of biliary tract anatomy and identification of liver tumor through the visualization of the disordered biliary excretion of ICG in real time. However, the actual efficacy of ICG-FNS to detect liver tumors is not clear. For example, false positive detection might occur because regenerative nodules develop as liver damage progresses¹⁶⁾. Also, small tumors located deep in the liver parenchyma might not be detected by this procedure.

Therefore, the aim of this study was to evaluate the actual efficacy of ICG-FNS in

cirrhotic or non-cirrhotic liver separately.

Materials and Methods

Patients

Ten cirrhotic whole livers were obtained from living donor liver transplant (LDLT) recipients. The original diseases included hepatitis C virus (HCV)-cirrhosis in 8, hepatitis B virus (HBV)-cirrhosis in 1, and alcoholic cirrhosis in 1. Patient characteristics are listed in Table 1. In addition, we evaluated twenty-three non-cirrhotic liver specimens obtained from patients who underwent hepatectomy for various kind of liver tumors [hepatocellular carcinoma (HCC) in 12, metastasis of colorectal cancer in 9, cholangiocarcinoma in 1, and hepatic carcinoid in 1] (Table 1).

Examination methods

As a fluorescence source, we used ICG (Diagnogreen, Daiichi Sankyo, Tokyo, Japan), which had been intravenously injected before surgery at a dose of 0.5mg per of body weight as part of a routine liver function test. The intervals between the ICG injection and surgery ranged from 2 days. As a fluorescent imaging tool, we used Photo Dynamic Eye-II (PDE-II, Hamamatsu Photonics, Hamamatsu, Japan), which filtered out light with a wavelength below 820 nm, and 36 light-emitting diodes with a wavelength of 760 nm. The camera imaging head was positioned between 20 and 30 cm above the

surgical specimen. The marking suture was performed near the site of the illuminated nodules during ten minutes while putting the emission of light situation in the video. Any illuminated nodules clearly visualized from the liver surface regardless of signal intensity, size and illuminated pattern were marked. The recognition of the illuminated nodules was clarified by two independent surgeons (T.T. and I. M.). Surgical specimens were observed from every angle, and cut to include each tumor's maximum diameter based on gross inspection. After the operation, the number of the illuminated lesions in the video and the number of the marking sites were counted and macroscopically analyzed. In addition, the number of illuminated lesions which were detected through the liver surface and the number of identifiable tumors by pathological examination were analyzed.

Statistical analysis

Results for continuous variables are expressed as the median (range). The positive predictive value was calculated as the number of pathological tumors in illuminated nodules. Data for continuous variables were compared using the Mann-Whitney U test. We set statistical significance at $p < .05$.

Results

The efficacy of ICG-FNS to detect HCCs in a cirrhotic liver

The median number of preoperatively detected tumors with various modalities in the 10 patients with cirrhotic liver was 2 (0-4). However, as shown in Figure 1, the median number of illuminated nodules was 20 (7-37), and the median number of nodules to be macroscopically considered as tumors was 16 (3-25). The number of pathologically diagnosed as tumors was 2 (0-8), so the positive predictive value was only 5.4% (0-24.2%). The number of false negatives was 14(4-17). There were significant differences between the numbers of preoperatively detected tumors and the number of both illuminated nodules and those macroscopically recognized as tumors, as shown in Figure 1 ($p < 0.001$). Moreover, there were also significant differences between the numbers of nodules pathologically diagnosed as tumors and the number of both illuminated nodules and nodules macroscopically recognized as tumors ($p < 0.001$). HCC on the liver surface with ICG-FNS revealed fluorescence in Fig 2A. The area that was actually illuminated was also macroscopically observed as HCC in Fig 2B. The same part was pathologically diagnosed as HCC in Fig 2C. However, the other areas that were illuminated and observed as nodules were diagnosed as regenerative nodules (Fig 2D-F).

The efficacy of ICG-FNS to detect malignant tumors in a non-cirrhotic liver

The median number of preoperatively detected tumors with various modalities

in twenty-three patients with non-cirrhotic liver was 1 (1-4). The median number of illuminated nodules and nodules macroscopically recognized as tumors was 1 (0-3) and 1 (1-4), respectively. Finally, the median number of nodules pathologically diagnosed as liver tumors was 1 (1-4), so that the positive predictive value to detect malignant tumors was 100%. There were no significant differences between the groups (Supplemental Figure 1). There was a significant difference in positive predictive value to detect HCC or malignant tumors between the cirrhotic livers and the non-cirrhotic livers (5.4% vs 100%; $p < 0.0001$). Although some tumors could be detected from the liver surface (Fig 3A, B) and positive predictive value to detect malignant tumors in the non-cirrhotic livers was 100%, other tumors could not be detected from the liver surface (11/34, 32.4%). These nodules were finally recognized after the liver was cut, including tumors (Fig 3C, D) and defined as non-illuminated nodules. There was a significant difference in the median depth from the liver surface between illuminated nodules ($n=23$) and non-illuminated nodules ($n=11$) (1.5mm vs 11.6mm, $p < 0.01$) (Fig 4A). Although there was no significant difference, non-illuminated nodules tended to be smaller than illuminated nodules (illuminated nodules, 32.4mm vs non-illuminated nodules, 20.7mm; $p=0.058$) (Fig 4B). Furthermore, the tumor size of almost all non-illuminated nodules located within 10mm depth tended to be smaller than 10mm (Figure 4C).

Discussion

ICG is usually used to directly measure the actual functional state of the liver

¹⁷⁾. ICG is a water-soluble, inert compound that is injected intravenously. It mainly binds to plasma proteins, is taken up by hepatocytes, and is excreted unchanged into the bile. Moreover, ICG is known to absorb infrared rays¹⁸⁾. Lights, and specially near-infrared light (NIR) in the biological window (700-900nm), can be exploited for intraoperative imaging guidance. Tanaka et al. demonstrated that (1) the appearance of the surgical field is not altered, (2) it is safe, (3) wavelengths in the 800nm range penetrate relatively deeply into living tissue, and (4) there has been a tremendous recent effort in developing general-purpose NIR fluorophores that can be conjugated to targeting or other molecules, thus creating “contrast agents” matched to any desired surgical application¹⁹⁾. Therefore, ICG injection combined with FNS is widely used to detect sentinel lymph nodes ⁴⁾⁻¹¹⁾, because this technique is convenient and safe for assessing lymph node status in the oncological field. Recently, adaptation of ICG-FNS was expanded further to hepatobiliary surgery and there have been some reports of its capability in detecting tumors ²⁾³⁾. Furthermore, several reports also showed that ICG-FNS was effective to check the bile leakage and the surgical margin ²⁾³⁾¹⁴⁾¹⁵⁾.

Our team sectioned whole livers with HCC removed from recipients who

underwent living donor liver transplantation and fully investigated them to detect small HCCs²⁰). Generally, hepatocytes have the ability to reproduce by themselves even if the hepatocytes are exposed to disorders. However, when hepatocytes are exposed to inflammation for a long time and repeatedly, hyperplasia of the collagen fiber deposits occurs strongly and many benign nodules, such as regenerative nodules, in a cirrhotic liver appear surrounded by collagen fiber in the extra-cellular matrix. In addition, the structure of the hepatic lobule is disturbed and the function of hepatocytes is affected²¹).

On the other hand, as described above, ICG binds to plasma proteins, one of which is ligandin. Ligandin is the binding protein of ICG and is uniformly distributed over hepatocytes in a normal liver. The expression of ligandin deviates with liver damage, and it is not expressed in areas of necrosis, fibrosis, or severe inflammation, so that the expression of ligandin becomes relatively rich in the regenerative area²²). Finally, the coloration of ICG is thought to accumulate in the regenerative nodules¹⁶). In fact, in our series of cirrhotic livers, many false positive nodules were illuminated, possibly because of the severe liver function disorder and the biliary excretion disorders²⁾¹⁶⁾²¹⁾²²).

However, Ishizawa et al. demonstrated that the signal intensity of the noncancerous liver parenchyma was higher in patients with an unfavorable ICG retention rate and in patients who had received the ICG injection within 24 hours before surgery²). Although

the interval longer than 2 days might be better to obtain a good lesion-to-liver contrast, especially in patients with advanced cirrhosis, we routinely perform the ICG test when the patients hospitalized generally 2 days before the operation. Also, the optimal interval between ICG injection and surgery to detect tumors remains controversial.

Secondly, we attempted to evaluate liver resection cases with non-cirrhotic livers. The aim of this study was to determine whether fluorescence navigation system was effective or not to detect tumors. Therefore, we did not evaluate the illuminated pattern of tumors. However, we got the same results as Ishizawa's report concerning with illuminated pattern of liver tumors (data not shown)²⁾. It was clear that although false positive nodules were not observed in the non-cirrhotic livers, smaller tumors and tumors that were located deeper than 10mm from liver surface to tumor were difficult to recognize as illuminated nodules. Kim et al have already described that near-infrared light penetrates human tissues to a depth of about 5-10 mm and Ishizawa et al. have also described that cancer detectability using fluorescent imaging technique seems mainly to depend on the depth of the tumors from the liver surface because of the limited tissue penetration of near-infrared light ²⁾²³⁾. Therefore, in our study, ICG-FNS wasn't able to detect tumors located deeper than 10mm. Possibly, 10mm is the maximum limit of depth for ICG-FNS to detect tumors. Based on these results, we suggested that the

capability of detecting tumors with ICG-FNS alone was not sufficient in both cirrhotic and non-cirrhotic livers.

We conclude that although ICG-FNS have the capability of detecting tumors and checking the bile leakage and surgical margin, it is necessary to know the limitation of ICG-FNS when searching liver malignancies in cirrhotic livers or small and deep liver malignancies in non-cirrhotic livers. Additional modalities including ultrasound should be adapted for use with this procedure to detect small liver tumors.

Author Contribution

Study design: Takayuki Tanaka

Acquisition of data: Takayuki Tanaka, Takanobu Hara, and Izumi Muraoka

Analysis and interpretation: Takayuki Tanaka, Mitsuhsa Takatsuki, Masaaki Hidaka,
and Akihiko Soyama

Manuscript drafted by: Takayuki Tanaka and Mitsuhsa Takatsuki

Revision: Takayuki Tanaka and Susumu Eguchi

Statistical Advice: Takayuki Tanaka, Tomohiko Adachi and Tamotsu Kuroki

Reference

1. Makuuchi M, Hasegawa H, Yamazaki S. Intraoperative ultrasonic examination for hepatectomy. *Ultrasound Med Biol.* 1983; Supple2: 493-497.

2. Ishizawa T, Fukushima N, Shibahara J, Masuda K, Tamura S, Aoki T, et al.
Real-time identification of liver cancers by using indocyanine green fluorescent imaging. *Cancer*. 2009; 115: 2491-2504.
3. Aoki T, Yasuda D, Shimizu Y, Odaira M, Niiya T, Kusano T, et al. Image-guided liver mapping using fluorescence navigation system with indocyanine green for anatomical hepatic resection. *World J Surg*. 2008; 32: 1763-1767.
4. Kitai T, Inamoto T, Miwa M, Shikayama T. Fluorescence navigation with indocyanine green for detecting sentinel lymph nodes in breast cancer. *Breast Cancer*. 2005; 12: 211-215.
5. Motomura K, Inaji H, Komoike Y, Kasugai T, Noguchi S, Koyama H. Sentinel node biopsy guided by indocyanine green dye in breast cancer patients. *Jpn Clin Oncol*. 1999; 29: 604-607.
6. Nimura H, Nariyama N, Mitsumori N, Yamazaki Y, Yanaga K, Urashima M.
Infrared ray electronic endoscopy combined with indocyanine green injection for detection of sentinel nodes of patients with gastric cancer. *Br J Surg*. 2004; 91: 575-579.
7. Kusano M, Tajima Y, Yamazaki K, Kato M, Watanabe M, Miwa M. Sentinel node mapping guided by indocyanine green fluorescence imaging: a new method for

- sentinel node navigation surgery in gastrointestinal cancer. *Dig Surg*. 2008; 25: 103-108.
8. Tajima Y, Yamazaki K, Masuda Y, Kato M, Yasuda D, Aoki T, et al. Sentinel node mapping guided by indocyanine green fluorescence imaging in gastric cancer. *Ann Surg*. 2009; 249: 58-62.
 9. Ito N, Fukuta M, Tokushima T, Nakai K, Ohgi S. Sentinel node navigation surgery using indocyanine green in patients with lung cancer. *Surg Today*. 2009; 34: 581-585.
 10. Soltesz EG, Kim S, Laurence RG, DeGrand AM, Parungo CP, Dor DM, et al. Intraoperative sentinel lymph node mapping of the lung using near-infrared fluorescent quantum dots. *Ann Thorac Surg*. 2005; 79: 269-277.
 11. Parungo CP, Ohnishi S, Kim SW, Kim S, Laurence RG, Soltesz EG, et al. Intraoperative identification of esophageal sentinel lymph nodes with near-infrared fluorescence imaging. *J Thorac Cardiovasc Surg*. 2005; 129: 844-850.
 12. Taggart DP, Choudhary B, Anastasiadis K, Abu-Omar Y, Balacumaraswami L, Pigott DW. Preliminary experience with a novel intraoperative fluorescence imaging technique to evaluate the patency of bypass grafts in total arterial revascularization. *Ann Thorac Surg*. 2003; 75: 870-873.

13. Detter C, Russ D, Iffland A, Wipper S, Schurr MO, Reichenspurner H, et al.
Near-infrared fluorescence coronary angiography: a new noninvasive technology for intraoperative graft patency control. *Heart Surg Forum*. 2002; 5: 364-369.
14. Ishizawa T, Tamaru S, Masuda K, Aoki T, Hasegawa K, Imamura H, et al.
Intraoperative fluorescent cholangiography using indocyanine green: a biliary road mapping for safe surgery. *J Am Coll Surg*. 2009; 208: 1-4.
15. Ishizawa T, Bandai Y, Kokudo N. Fluorescent cholangiography using indocyanine green for laparoscopic cholecystectomy: an initial experience. *Arch Surg*. 2009; 144: 381-382.
16. Lin WR, Lim SN, Macdonald SA, Graham T, Wright VL, Peplow CL, et al. The histogenesis of regenerative nodules in human liver cirrhosis. *Hepatology*. 2010; 51: 1017-1026.
17. Makuuchi M, Kosyga T, Takayama T, Yamazaki S, Kakazu T, Miyagawa S, et al.
Surgary for small liver cancers. *Semin Surg Oncol*. 1993; 9: 298-304.
18. Ohkubo H, Musha H, Okuda H. Effects of caloric restriction on the kinetics of indocyanine green in patients with liver diseases and in the rat. *Am J Dig Dis*. 1978; 23: 1017-1024.
19. Tanaka E, Choi HS, Fujii H, Bawendi MG, Frangioni JV. Image-guided oncologic

- surgery using invisible light: completed pre-clinical development for sentinel lymph node mapping. *Ann Surg Oncol*. 2006; 13: 1671-1681.
20. Hidaka M, Eguchi S, Okudaira S, Takatsuki M, Tokai H, Soyama A, et al. Multicentric occurrence and spread of hepatocellular carcinoma in whole explanted end-stage liver. *Hepatol Res*. 2009; 39 : 143-148.
21. Nakanuma Y. Non-neoplastic nodular lesions in the liver. *Pathol Int*. 1995; 45: 7013-714.
22. Sathirakul K, Suzuki H, Yasuda K, Hanano M, Tagaya O, Horie T, et al. Kinetic analysis of hepatobiliary transport of organic anions in Eisai hyperbilirubinemic mutant rats. *J Pharmacol Exp Ther*. 1993; 265: 1301-1312.
23. Kim S, Lim YT, Soltesz EG, De Grand AM, Lee J, Nakayama A et al. Near-infrared fluorescent type II quantum dots for sentinel lymph node mapping. *Nat Biotechnol*. 2004; 22: 93-97.

Figure Legends

Figure 1: The number of detected nodules in a cirrhotic liver

The median number of preoperative, illuminated, macroscopic, pathological tumors with cirrhotic liver was, in order, 2 (0-4), 20 (7-37), 16 (3-25), and 2 (0-8). There were significant differences between preoperative tumors and both illuminated nodules and macroscopic tumor ($p < 0.001$). Moreover, there were also significant differences between pathological tumor and both illuminated nodules and macroscopic tumor ($p < 0.001$).

Figure 2: ICG-FNS for patients with cirrhotic liver and pathological results

A, HCCs on the liver surface with ICG-FNS revealed the illuminated nodules. B, The area that actually emitted light was also macroscopically observed as liver tumor. C, The same area was pathologically diagnosed as HCC. D, The other areas on the liver surface in the same case also revealed the illuminated nodules. E, The areas that emitted light were macroscopically observed as nodules. F, Finally, these areas were diagnosed as regenerative nodules.

Figure 3: ICG-FNS for patients with liver resection with non-cirrhotic liver.

Liver tumors in illuminated nodules could be observed as illuminated nodules on the liver surface (Figure 3A-B); liver tumors in non-illuminated nodules could not be

observed as illuminated lesions on the surface, and finally recognized after the liver was cut including the tumor under US guidance (Fig3C-D).

Figure 4: Comparison between illuminated nodules and non-illuminated nodules on the liver surface in a non-cirrhotic liver

A: There was a significant difference in median depth from the liver surface between illuminated nodules and non-illuminated nodules (1.5mm vs 11.6mm, $p < 0.01$). B:

Non-illuminated nodules tended to be smaller than illuminated nodules (illuminated nodules, 32.4mm vs non-illuminated nodules, 20.7mm; $p = 0.058$). C: Correlation

diagram of the depth and tumor size presented. The tumor size of almost all

non-illuminated nodules located within 10mm depth tended to be smaller than 10mm.

Supplemental Figure 1: Number of detected nodules in a non-cirrhotic liver

The median number of preoperative, illuminated, macroscopic, and pathological tumors with non-cirrhotic liver was, in order, 1 (1-4), 1 (0-3), 1 (1-4), and 1 (1-4). There were no significant differences in each group.

Table 1: The characteristics of patients with a cirrhotic liver and a non-cirrhotic liver

	cirrhotic liver for LDLT (n=10)	non-cirrhotic liver for liver resection (n=23)
Gender (Male: Female)	6:4	16:7
Age*	61(38-72)	67.5(60-90)
liver disease	HCV:8, HBV:1,alcohol:1	HCV:5, HBV:5, NBNC:4, NL:9
liver tumor	HCC:9	HCC:12, metastases : 9, CCC : 1, Carcinoid : 1
Total-bilirubin(mg/dl)*	3.2(0.5-8.8)	0.8(0.3-1.4)
AST(IU/l)*	52(30-89)	28(13-285)
ALT(IU/l)*	29(15-75)	27(10-100)
Albumin(g/dl)*	2.6(2.1-3.8)	4.2(2.9-5.2)
Platetlet(x10 ⁴ /mm ³)*	6.4(2.3-13.4)	16.4(10.8-27.6)
PT(INR)*	1.47(1.07-1.95)	1.00(0.87-1.13)
ICGR15(%)*	44(24-70)	11(2-15)
Child-Pugh score*	9(5-12)	5(5-7)
MELD score*	14(7-22)	-

HCV: Hepatitis C virus, HBV: Hepatitis B virus, NBNC:non-HBV non HCV,
 NL: normal liver, HCC: Hepatocellular carcinoma, CCC: cholangiocarcinoma,
 AST: aspartate aminotransferase, ALT: alanine aminotransferase,
 PT: prothrombin time, INR: international normalized ratio,
 ICGR15: indocyanine green retention rate at 15 minutes,
 MELD score: model for endstage liver disease score
 *median (range)

Figure 1: The number of detected nodules in a cirrhotic liver.

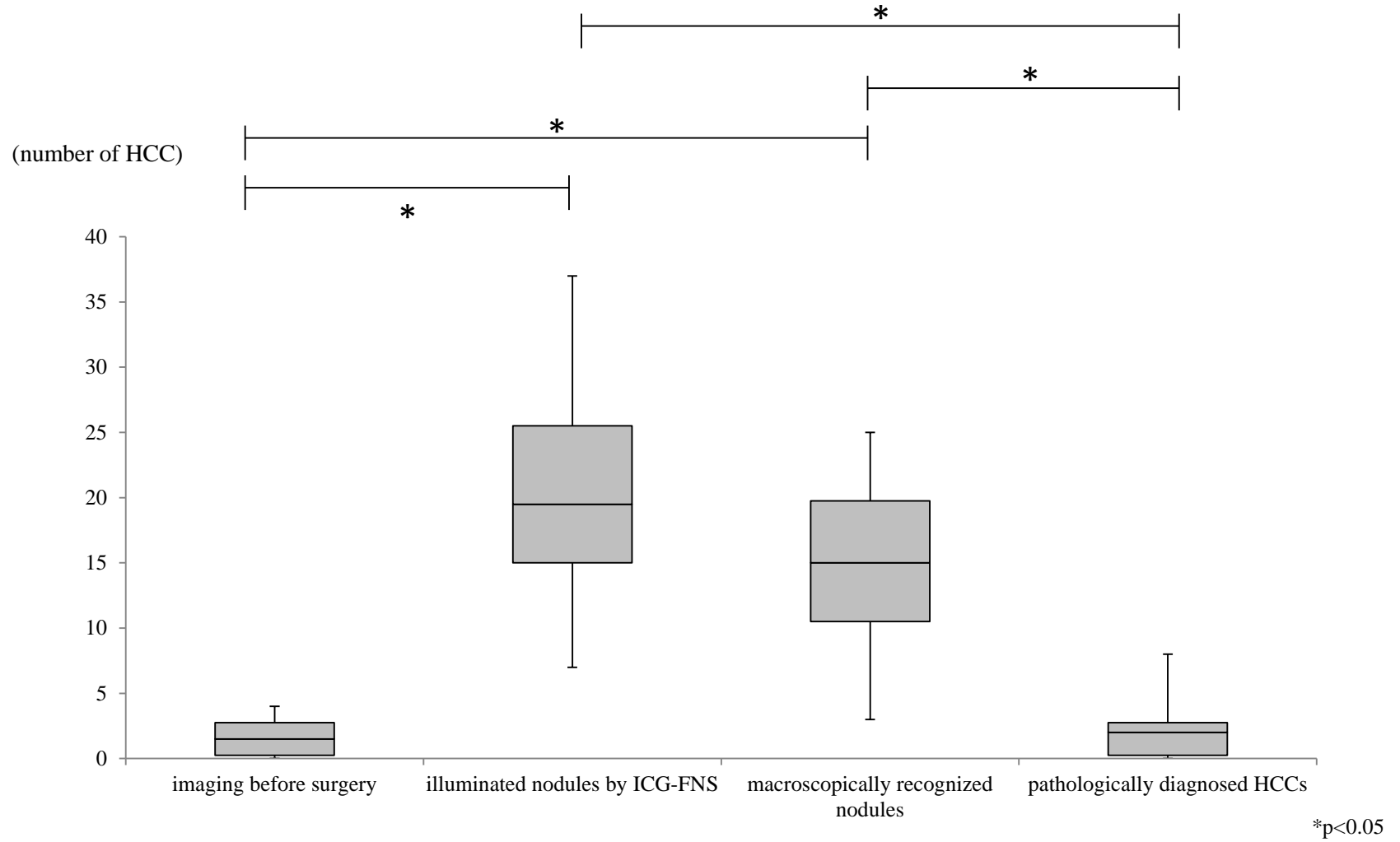


Figure 2: ICG-FNS for patients with cirrhotic liver and pathological results.

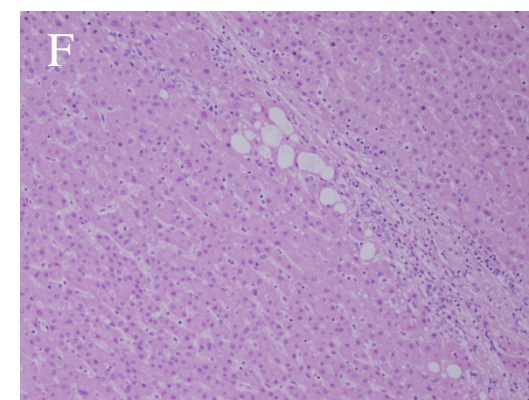
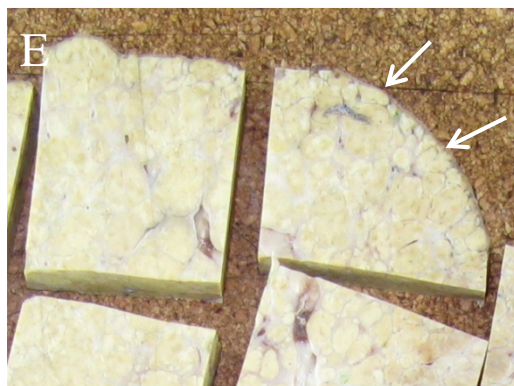
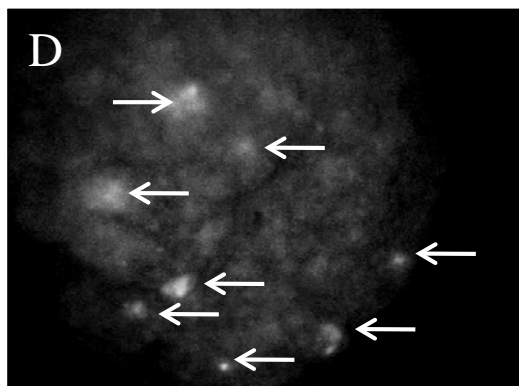
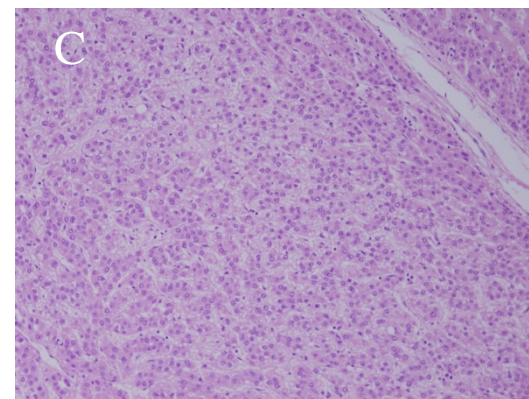
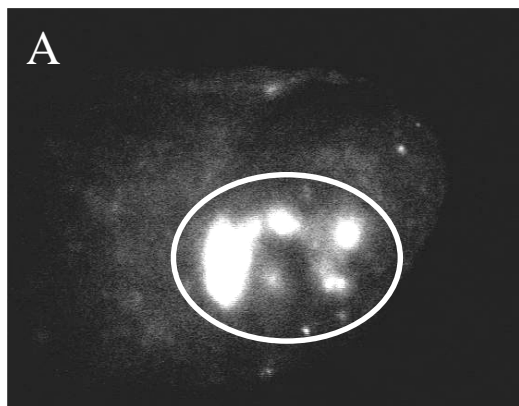


Figure 3: ICG-FNS for patients with liver resection with non-cirrhotic liver.

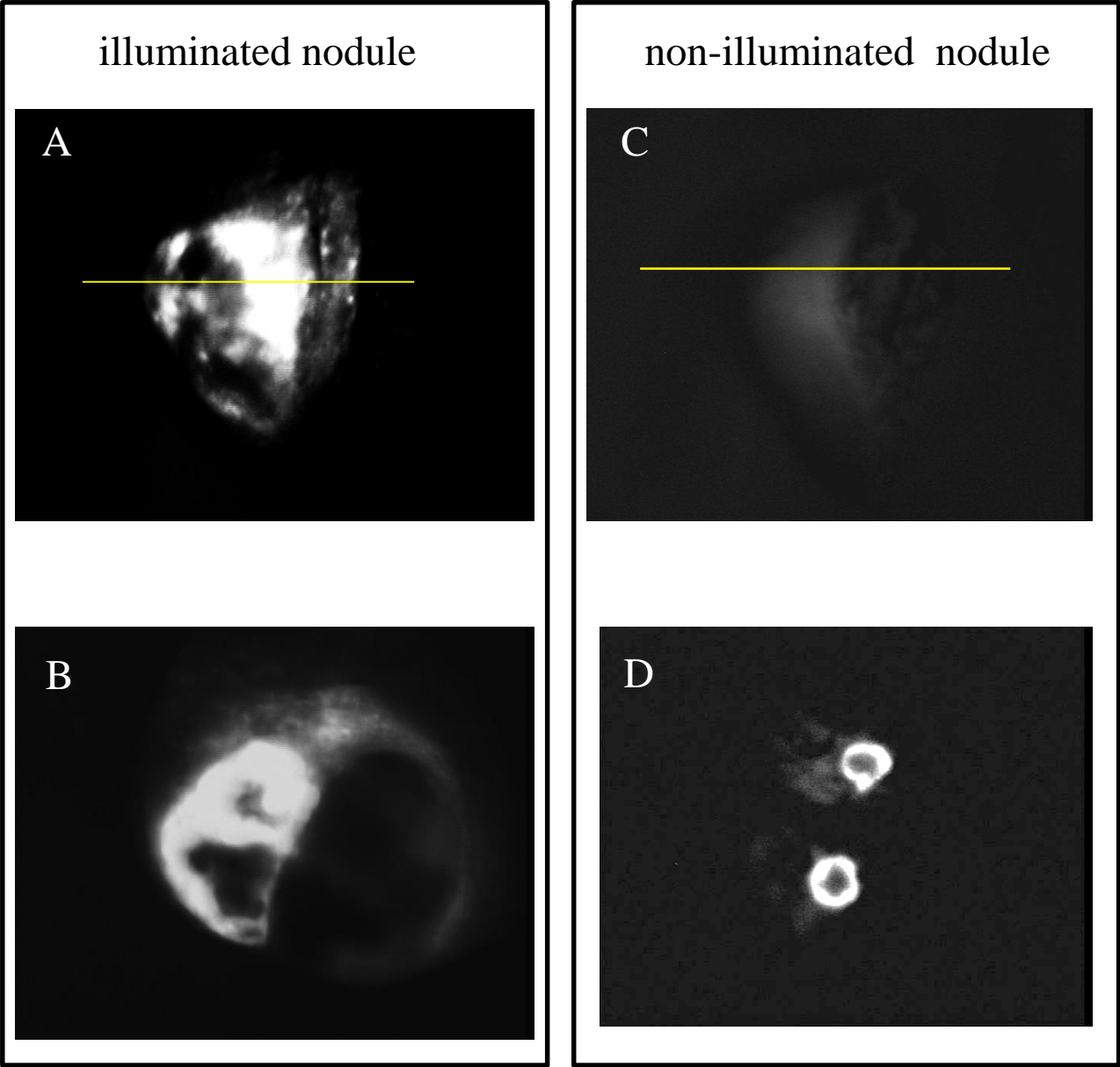
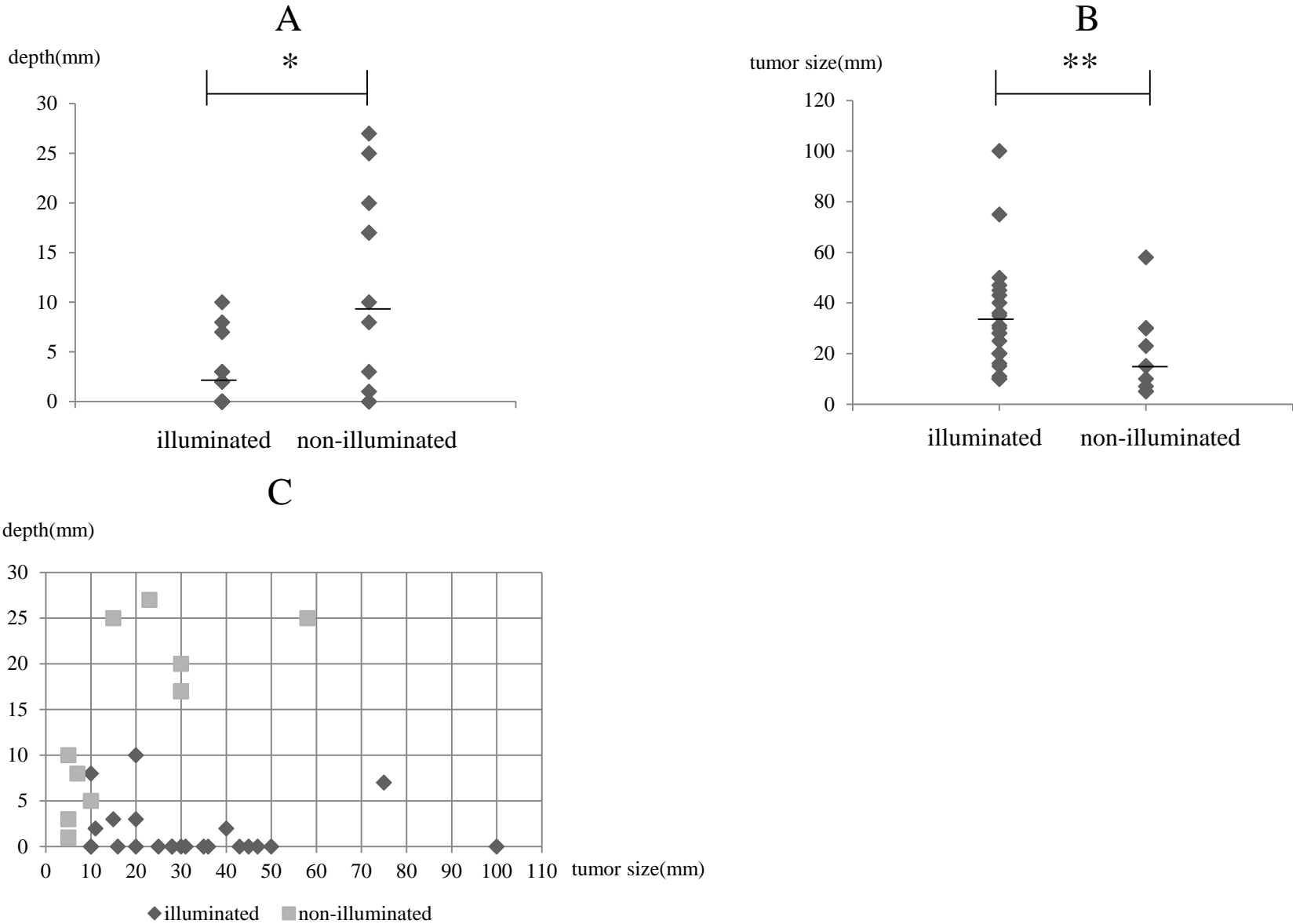


Figure 4: The comparison between illuminated nodules and non-illuminated nodules on the liver surface in a non-cirrhotic liver.



*p<0.01 **p=0.058

Supplemental figure: The number of detected nodules in a non-cirrhotic liver.

